Estimating Optimal Tracking Filter Performance for Manned Maneuvering Targets

ROBERT A. SINGER, Member, IEEE
Hughes Aircraft Company
Ground Systems Group
Fullerton, Calif. 92634

Abstract

The majority of tactical weapons systems require that manned maneuverable vehicles, such as aircraft, ships, and submarines, be tracked accurately. An optimal Kalman filter has been derived for this purpose using a target model that is simple to implement and that represents closely the motions of maneuvering targets. Using this filter, parametric tracking accuracy data have been generated as a function of target maneuver characteristics, sensor observation noise, and data rate and that permits rapid a priori estimates of tracking performance to be made when maneuvering targets are to be tracked by sensors providing any combination of range, bearing, and elevation measurements.

I. Introduction

Most tactical weapons systems require accurate tracking of manned maneuverable vehicles such as aircraft, ships, and submarines. Although much attention has been given in the literature to tracking orbital, suborbital, and reentering targets, little [1], [2] has been given to this important problem of tracking piloted threats. This paper treats this problem by first developing a simple target model that closely represents the ensemble behavior of different maneuvering vehicles and that when used in the appropriate Kalman filter yields a tracking algorithm that provides optimal performance for this class of targets and that is easily implemented.

The design and analysis of weapons systems often requires determining the expected tracking accuracies against maneuvering targets of various types. Generally this task is time consuming and the results are often limited to specific targets, sensors, and environments. This paper, by secondly presenting tracking accuracy figures parametrically as a function of target maneuver characteristics, observation noise, and data rate, permits, by interpolation, an accurate estimation of optimal tracking performance to be made rapidly. The results are presented for a single physical dimension to facilitate adaption to the range-bearing, range-bearing-elevation, and bearing-elevation sensor measurement sets that are often provided by any of radar, sonar, and IR sensors.

The results in this paper also indicate the sensitivity of tracking accuracy to the primary tracking parameters, and how to select data rates to obtain desired filtering accuracies.

II. Dynamic Equations of Target Motion

The target model selected for tracking applications must be sufficiently simple to permit ready implementation in weapons systems for which computation time is at a premium yet sufficiently sophisticated to provide satisfactory tracking accuracy. The model presented in this section satisfies both of these objectives and certain variations have already been selected for implementation in modern tactical weapon systems and have had their theoretical performance figures verified by Monte Carlo simulation techniques using realistic target trajectories.

The model is based on the fact that, without maneuvering, manned vehicles of the class under consideration (such as aircraft, ships, and submarines) generally follow straight line constant velocity trajectories. If the vehicles were not able to deviate from these trajectories, i.e., could not maneuver, then the tracking problem could be solved quickly and simply using standard filtering algorithms such as least squares, polynomial fitting, and α-β techniques. However, the maneuver capability of these vehicles constitute the single feature that makes these algorithms generally unsuitable for accurate tracking. The target model presented here accounts for this

Manuscript received December 4, 1969.

maneuver capability in a way that is simple and that provides a suitable representation of the maneuver phenomena.

The model differs from those discussed in [1] and [2] in two important ways. First, the maneuver equations are derived for the actual continuous time target motion and are then expressed in discrete time according to the standard discretization procedure, thereby providing accurate statistical representation of the true target behavior. Formerly, the equations were derived originally in discrete time and, as a result, distorted somewhat certain aspects of the continuous time target motion. Second, the dimension of the model is three states (per Cartesian axis) rather that four as in [1]. The number of independent elements of the covariance matrix has therefore been reduced from ten to six, permitting greater implementational ease. Despite the reduction in dimension, the resulting performance is significantly greater (≥ 30 percent in most cases) for the target class under consideration. This occurs because the model in [1] assumes a constant acceleration trajectory for the nonmaneuver norm while the model here assumes a constant velocity trajectory for the norm. The latter trajectory, which is the important special case of the former for which the constant acceleration is known to be zero, contains more target information and is more applicable to aircraft, ship, and submarine targets.

The model below is presented for a single spatial dimension (such as x, y, range, bearing, or elevation) in order to enable accurate tracking performance estimates to be made for a variety of sensor measurement sets. For example, if a radar provides range and bearing measurements, target tracking could be performed in the coordinates defined by the range and bearing directions, and the parametric data presented later in the report could be evaluated for tracking in each of the range and bearing directions separately and then appropriately root-sum-squared to obtain reliable estimates of position and speed errors for this situation. This procedure will be illustrated later in this paper. Similar procedures would be followed for other sets of sensor measurements.

The targets under consideration normally move at constant velocity. Turns, evasive maneuvers, and accelerations due to atmospheric turbulence may be viewed as perturbations upon the constant velocity trajectory. In a single physical dimension, the target equations of motion may be represented by

$$\dot{x}'(t) = F'x'(t) + G'a(t) \tag{1}$$

where

$$\begin{bmatrix} 0 & 1 \\ 0 & 0 \end{bmatrix}\begin{bmatrix} x \\ \dot{x} \end{bmatrix} + \begin{bmatrix} 0 \\ 1 \end{bmatrix}$$

$$x'(t) = \begin{cases} \text{target position at time } t \\ \text{target speed at time } t \end{cases}$$

$a(t) =$ target acceleration at time t

$$F' = \begin{bmatrix} 0 & 1 \\ 0 & 0 \end{bmatrix}, \qquad G' = \begin{bmatrix} 0 \\ 1 \end{bmatrix}.$$

$$\begin{bmatrix} \dot{x} \\ 0 \end{bmatrix}$$

The acceleration $a(t)$, since it accounts for the target deviations from a straight line trajectory, will henceforth be termed the target maneuver variable. The (single dimension) maneuver capability can be satisfactorily specified by two quantities: the variance, or magnitude, of the target maneuver and the time constant, or duration, of the target maneuver.

The target acceleration, and hence the target maneuver, is correlated in time; namely, if a target is accelerating at time t, it is likely to be accelerating at time $t+\tau$ for sufficiently small τ. For example, a lazy turn will often give rise to correlated acceleration inputs for up to one minute, evasive maneuvers will provide correlated acceleration inputs for periods between ten and thirty seconds, and atmospheric turbulence may provide correlated acceleration inputs for one or two seconds. A typical representative model of the correlation function $r(\tau)$ associated with the target acceleration is

$$r(\tau) = Ea(t)a(t+\tau) = \sigma_m^2 e^{-\alpha|\tau|}, \quad \alpha \geq 0 \tag{2}$$

where σ_m^2 is the variance of the target acceleration and α is the reciprocal of the maneuver (acceleration) time constant. For example, $\alpha \simeq 1/60$ for a lazy turn, $\simeq 1/20$ for an evasive maneuver, and $\simeq 1$ for atmospheric turbulence. Fig. 1 illustrates the correlation function.

The variance σ_m^2 of target acceleration is calculated using the model illustrated in Fig. 2. The target can accelerate at a maximum rate A_{max} ($-A_{max}$) and will do each with a probability P_{max}. The target undergoes no acceleration with a probability P_0, and will accelerate between the limits $-A_{max}$ and A_{max} according to the appropriate uniform distribution. The variance σ_m^2 of the resulting acceleration probability density model is

$$\sigma_m^2 = \frac{A_{max}^2}{3}\left[1 + 4P_{max} - P_0\right].$$

This model has been utilized in tracking simulations and has been shown to provide a satisfactory representation of the target's instantaneous maneuver characteristics.

Utilizing the correlation function $r(\tau)$, the acceleration $a(t)$ may be expressed in terms of white noise by the Wiener–Kolmogorov whitening procedure [3]. The Laplace transform of $r(\tau)$ given by

$$R(s) = \mathcal{L}\{r(\tau)\} = \frac{-2\alpha\sigma_m^2}{(s-\alpha)(s+\alpha)} = H(s)H(-s)W(s) \tag{3}$$

where

$$H(s) = \frac{1}{s+\alpha}$$
$$W(s) = 2\alpha\sigma_m^2. \tag{4}$$

The quantity $H(s)$ is the transform of the whitening filter for $a(t)$, and $W(s)$ is the transform of the white noise $w(t)$ that drives $a(t)$. The resulting equations are therefore

$$\dot{a}(t) = -\alpha a(t) + w(t) \tag{5}$$

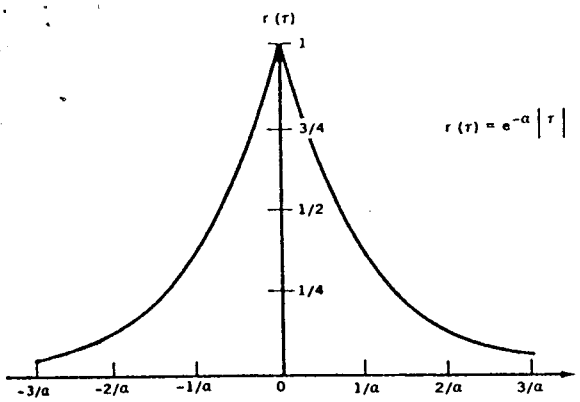

Fig. 1. Correlation function of target acceleration.

Fig. 2. Model of the target acceleration probability density.

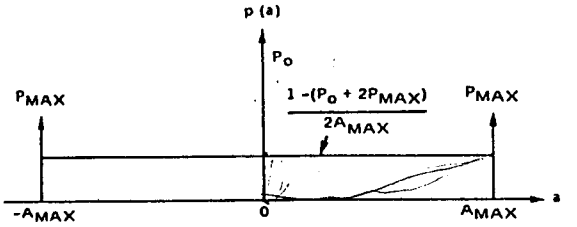

where $\sigma_w^2(\tau)$, the correlation function of the white noise input, satisfies

$$\sigma_w^2(\tau) = 2\alpha\sigma_m^2\delta(\tau). \tag{6}$$

The target equations of motion (in one dimension) can now be expressed in terms of the white noise $w(t)$ as follows:

$$\dot{x}(t) = Fx(t) + Gw(t)$$

where

$$x(t) = \begin{cases} \text{target position at time } t \\ \text{target speed at time } t \\ \text{target acceleration at time } t \end{cases} \tag{7}$$

$w(t)$ = white noise driving function with variance $2\alpha\sigma_m^2$

III. Discrete Time Equations of Motion

Many sensors have a constant data rate, sampling target position every T seconds. The appropriate (discrete time) target equations of motions for this application are given by

$$x(k+1) = \Phi(T, \alpha)x(k) + u(k) \tag{8}$$

where $\Phi(T, \alpha)$ is the target state transition matrix and $u(k)$ is the inhomogeneous driving input. This input is not a sampled version of the continuous time white noise input $w(t)$, although $u(k)$ will be shown subsequently to be white in the discrete time sense. Since

$$x(t+T) = e^{FT}x(t) + \int_t^{t+T} e^{F(t+T-\tau)}Gw(\tau)d\tau \tag{9}$$

it follows that for the model (7),

$$\Phi(T, \alpha) = e^{FT}$$

$$u(k) = \int_{kT}^{(k+1)T} \exp\{F[(k+1)T - \tau]\}Gw(\tau)d\tau. \tag{10}$$

These terms can be calculated using eigenvalue analysis. The eigenvalues of F satisfy

$$\det(\lambda I - F) = \lambda^2(\lambda + \alpha) = 0 \tag{11}$$

so that

$$\lambda = \{0, 0, -\alpha\}. \tag{12}$$

It can be verified that

$$\Phi(T, \alpha) = \begin{bmatrix} 1 & T & \frac{1}{\alpha^2}[-1 + \alpha T + e^{-\alpha T}] \\ 0 & 1 & \frac{1}{\alpha}[1 - e^{-\alpha T}] \\ 0 & 0 & e^{-\alpha T} \end{bmatrix}. \tag{13}$$

When αT is small, $\Phi(T, \alpha)$ reduces to the Newtonian matrix

$$\Phi = \begin{bmatrix} 1 & T & T^2/2 \\ 0 & 1 & T \\ 0 & 0 & 1 \end{bmatrix}. \tag{14}$$

The input vector $u(k)$ satisfies

$$u(k) = \int_{kT}^{(k+1)T} \begin{bmatrix} 1 & (k+1)T - \tau & 1/\alpha^2\{-1 + \alpha((k+1)T - \tau) + \exp[-\alpha((k+1)T - \tau)]\} \\ 0 & 1 & 1/\alpha\{1 - \exp[-\alpha((k+1)T - \tau)]\} \\ 0 & 0 & \exp[-\alpha((k+1)T - \tau)] \end{bmatrix} \begin{bmatrix} 0 \\ 0 \\ 1 \end{bmatrix} w(\tau)d\tau$$

$$= \int_{kT}^{(k+1)T} \begin{bmatrix} 1/\alpha^2\{-1 + \alpha((k+1)T - \tau) + \exp[-\alpha((k+1)T - \tau)]\} \\ 1/\alpha\{1 - \exp[-\alpha((k+1)T - \tau)]\} \\ \exp[-\alpha((k+1)T - \tau)] \end{bmatrix} w(\tau)d\tau = \int_{kT}^{(k+1)T} \begin{bmatrix} n_1(\tau) \\ n_2(\tau) \\ n_3(\tau) \end{bmatrix} w(\tau)d\tau. \tag{15}$$

$$F = \begin{bmatrix} 0 & 1 & 0 \\ 0 & 0 & 1 \\ 0 & 0 & -\alpha \end{bmatrix}, \qquad G = \begin{bmatrix} 0 \\ 0 \\ 1 \end{bmatrix}.$$

Since $w(t)$ is white noise, $E[u(k)u(k+i)] = 0$ for $i \neq 0$ so that $u(k)$ is a discrete time white noise sequence. The state equations just derived are therefore directly suitable for Kalman filter applications.

IV. Kalman Filter Equations

The tracking sensor measures target position (x, y, range, bearing, or elevation) along the dimension being analyzed and provides the following output equation:

$$y(k) = Hx(k) + v(k) \tag{16}$$

where

$$H = [1\ 0\ 0]$$

and $v(k)$ is additive white noise with variance σ_R^2.

Equations (8) and (16) with $\phi(T, \alpha)$ given by (13) and $u(k)$ by (15) have the form for which the optimal linear filter is identically the Kalman filter. Other filters can of course be used to estimate the target state vector $x(k)$; however, the Kalman filter provides the best performance in terms of minimizing the mean square estimation error, it can generally be easily implemented, and, even when it cannot, it provides useful upper bounds to tracking filter performance.

The Kalman filter state equations are [4]

$$\begin{aligned}\hat{x}(k+1/k) &= \Phi(T, \alpha)\hat{x}(k/k)\\ \hat{x}(k/k) &= \hat{x}(k/k-1)\\ &\quad + P(k/k-1)H^T[HP(k/k-1)H^T + \sigma_R^2]^{-1}\\ &\quad \cdot [y(k) + H\hat{x}(k/k-1)],\end{aligned} \tag{17}$$

where

$\hat{x}(k/k)$ = minimum mean square estimate of $x(k)$ given sensor data up to and including time k; i.e., the filtered estimate,

$\hat{x}(k+1/k)$ = minimum mean square estimate of $x(k+1)$ given sensor data up to and including time k; i.e., the one-sample-ahead prediction.

The matrices $P(k/k)$ and $P(k/k-1)$ are the covariance matrices of the filtered and one-sample-ahead prediction errors, respectively. These matrices satisfy the following recursion equations:

$$\begin{aligned}P(k/k-1) &= \Phi(T, \alpha)P(k-1/k-1)\Phi^T(T, \alpha) + Q(k)\\ P(k/k) &= P(k/k-1)\\ &\quad - P(k/k-1)H^T[HP(k/k-1)H^T + \sigma_R^2]^{-1}\\ &\quad \cdot HP(k/k-1).\end{aligned} \tag{18}$$

The matrix $Q(k)$ is the maneuver excitation covariance matrix and, as shown in Appendix I, has the form

$$Q(k) = E[u(k)u^T(k)] = 2\alpha\sigma_m^2 \begin{bmatrix} q11 & q12 & q13 \\ q12 & q22 & q23 \\ q13 & q23 & q33 \end{bmatrix} \tag{19}$$

where

$$\begin{aligned}q11 &= \frac{1}{2\alpha^5}\left[1 - e^{-2\alpha T} + 2\alpha T + \frac{2\alpha^3T^3}{3} - 2\alpha^2T^2 - 4\alpha Te^{-\alpha T}\right]\\ q12 &= \frac{1}{2\alpha^4}\left[e^{-2\alpha T} + 1 - 2e^{-\alpha T} + 2\alpha Te^{-\alpha T} - 2\alpha T + \alpha^2T^2\right]\\ q13 &= \frac{1}{2\alpha^3}\left[1 - e^{-2\alpha T} - 2\alpha Te^{-\alpha T}\right]\\ q22 &= \frac{1}{2\alpha^3}\left[4e^{-\alpha T} - 3 - e^{-2\alpha T} + 2\alpha T\right]\\ q23 &= \frac{1}{2\alpha^2}\left[e^{-2\alpha T} + 1 - 2e^{-\alpha T}\right]\\ q33 &= \frac{1}{2\alpha}\left[1 - e^{-2\alpha T}\right].\end{aligned} \tag{20}$$

For a fixed sensor and target class, the quantities α and T are fixed so that $Q(k)$ is a constant matrix. When T is sufficiently small so that $\alpha T \ll \frac{1}{2}$,

$$\lim_{\alpha T \to 0} Q(k) = 2\alpha\sigma_m^2 \begin{bmatrix} T^5/20 & T^4/8 & T^3/6 \\ T^4/8 & T^3/3 & T^2/2 \\ T^3/6 & T^2/2 & T \end{bmatrix} \tag{21}$$

reflecting the fact that for sufficiently short time periods the physical target moves at essentially constant velocity. For a fixed sampling rate, as $\alpha \to \infty$,

$$\lim_{\alpha \to \infty} Q(k) = \begin{bmatrix} 0 & 0 & 0 \\ 0 & 0 & 0 \\ 0 & 0 & \sigma_m^2 \end{bmatrix}. \tag{22}$$

The Kalman filter equations (17) are initialized by

$$\begin{aligned}\hat{x}_1(1/1) &= y(1)\\ \hat{x}_2(1/1) &= [y(1) - y(0)]/T\\ \hat{x}_3(1/1) &= 0\end{aligned} \tag{23}$$

where $y(0)$ and $y(1)$ are, respectively, the first and second sensor measurements received. The corresponding covariance initialization equations for (18) are, as shown in Appendix II,

$$\begin{aligned}P11(1/1) &= \sigma_R^2\\ P12(1/1) &= P21(1/1) = \sigma_R^2/T\\ P13(1/1) &= P31(1/1) = 0\\ P22(1/1) &= 2\sigma_R^2/T^2 + \frac{\sigma_M^2}{\alpha^4T^2}\left[2 - \alpha^2T^2 + \frac{2\alpha^3T^3}{3} - 2e^{-\alpha T} - 2\alpha Te^{-\alpha T}\right]\\ P23(1/1) &= P32(1/1) = \frac{\sigma_M^2}{\alpha^2T}\left[e^{-\alpha T} + \alpha T - 1\right]\\ P33(1/1) &= \sigma_M^2.\end{aligned} \tag{24}$$

When, as is often the case, acquisition of the target occurs before the target commences maneuvering, the covariance initialization equations (24) reduce to

$$\begin{aligned}P11(1/1) &= \sigma_R^2\\ P12(1/1) &= P21(1/1) = \sigma_R^2/T\\ P22(1/1) &= 2\sigma_R^2/T^2\\ P13(1/1) &= P31(1/1) = P23(1/1)\\ &= P32(1/1) = P33(1/1) = 0.\end{aligned} \tag{25}$$

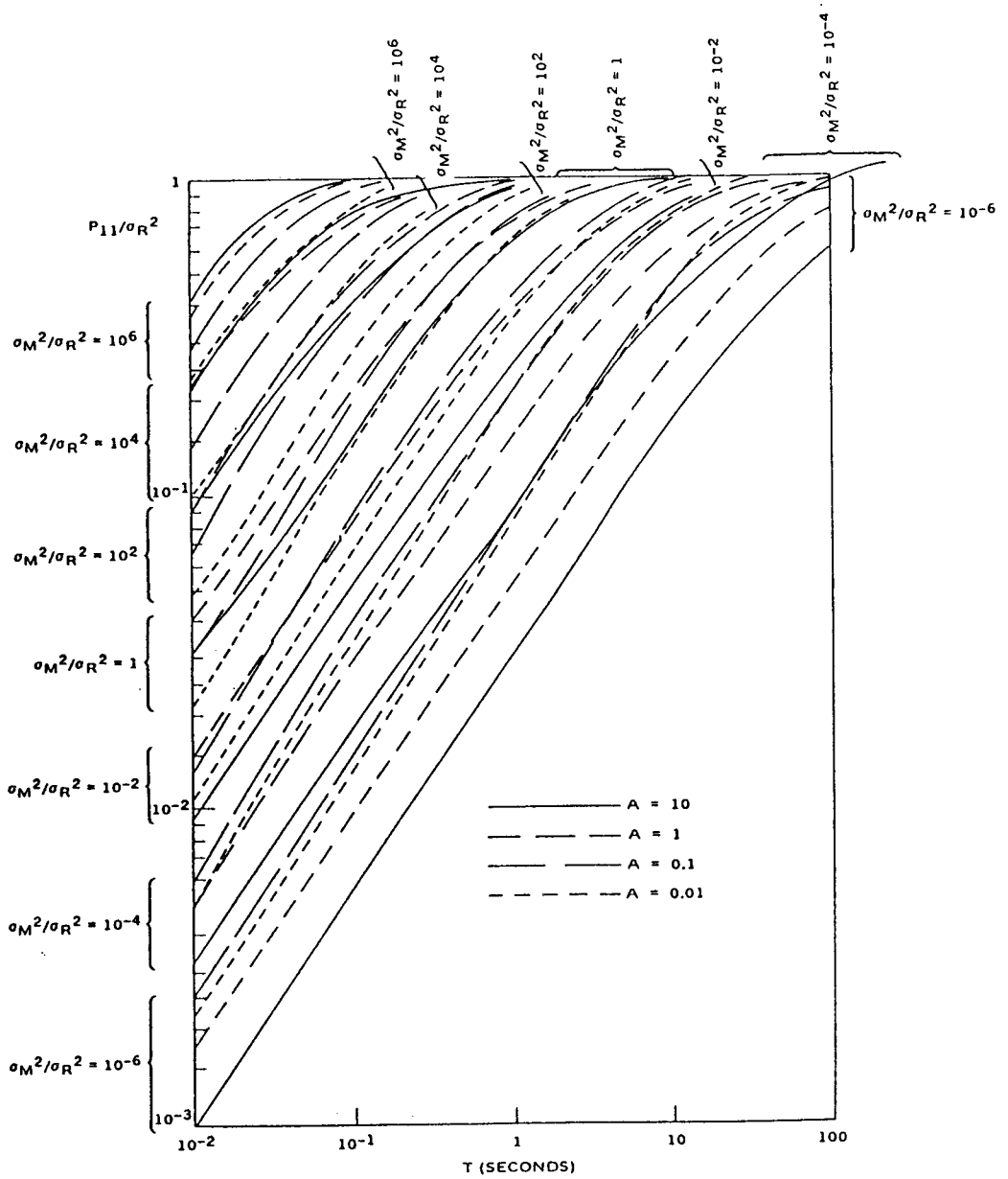

Fig. 3. Parametric behavior of P_{11}, the variance of the filtered position error.

V. Estimating Tracking Performance Using Parametric Data

The Kalman filter recursion equations (18) were exercised for a spectrum of values of sampling interval (T), maneuver magnitude (σ_M^2), maneuver correlation coefficient (α), and sensor observation noise (σ_R^2). Figs. 3, 4, and 5 compactly illustrate the parametric behavior of three important steady-state filtering errors for sampling intervals between 0.01 and 100 seconds, for σ_M^2/σ_R^2 ratios of 10^i for i between -6 and 6, and for correlation coefficient values of 0.01, 0.1, 1, and 10. These parameter values span the spectrum of values that can occur during tactical encounters. As shown in [5] the covariance matrix P is a function of σ_R^2, σ_M^2, α, and T such that P/σ_R^2 is a function only of σ_M^2/σ_R^2, α, and T. This has been verified by computer analysis and has been used to reduce the tracking data to the form shown in Figs. 3, 4, and 5. In these figures, the correlation coefficient α is denoted by A. The elements P_{ij} of the steady filter covariance matrix provide the statistics of the tracking errors. The term P_{ij}, for example, is $E[\varepsilon_{x_i}\varepsilon_{x_j}]$. Thus P_{11}, P_{22}, and P_{33} are the variances, respectively, of the filtered position, speed, and acceleration errors along the single dimension being analyzed. Similarly the quantities P_{12}, P_{13}, and P_{23} are the covariances, respectively, between the filtered position and velocity errors, the position and acceleration errors, and the velocity and acceleration errors.

The statistics provided by the covariance matrix are those that result when the target model and system parameters used in the Kalman filter correspond closely to those of the physical encounter. Hence tests must be conducted to determine whether or not the empirical, or actual, tracking statistics compare favorably with the theoretical statistics obtained from the Kalman filter equations. Although such a comparison has not been performed in detail for the model presented in this paper,

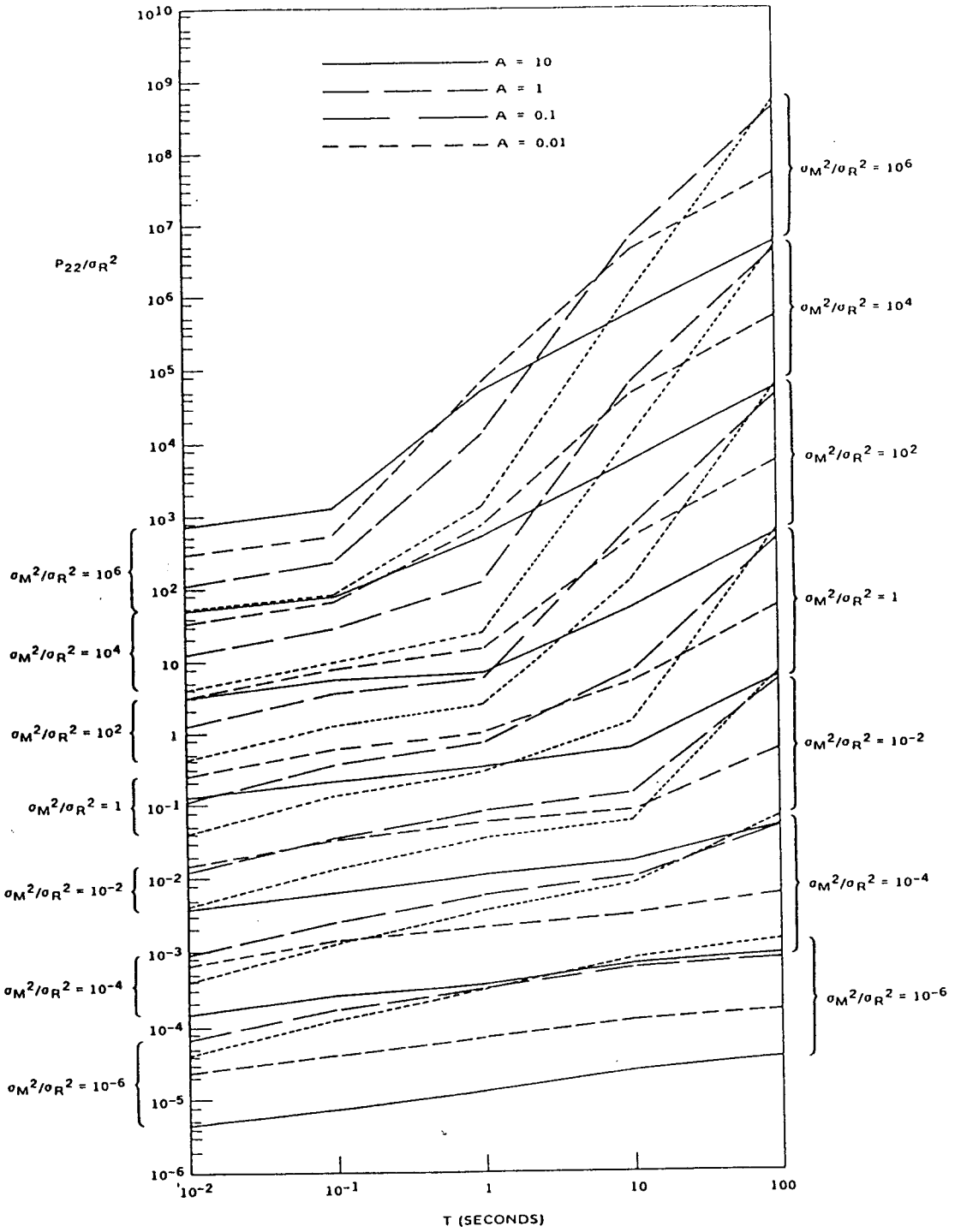

Fig. 4. Parametric behavior of P_{22}, the variance of the filtered velocity error.

onte Carlo trials for a spectrum of target vehicles, en-unter geometries, sensor classes, and environments ve illustrated agreement to within 30 percent between e theoretical and empirical tracking accuracies ob-ined with a similar, but not identical, model.

Fig. 3 gives the parametric behavior of the ratio $_1/\sigma_R^2$, which is the ratio of the variance of the steady-ate error in filtered position to the variance of the single-ok sensor observation noise. This ratio represents the nprovement in position tracking resulting from using e optimal filter rather than the raw sensor measure-ents directly. When this ratio is close to unity, the accuracy improvement provided by the filter is small. As the ratio decreases toward zero, the filter becomes increasingly effective.

Fig. 4 gives the parametric behavior of P_{22}/σ_R^2, the ratio of the variance of the steady-state error in filtered speed along the given dimension to the variance of the observation noise in that dimension. Fig. 5 illustrates the parametric behavior of P_{12}/σ_R^2, where, as discussed earlier, P_{12} is the covariance between the steady-state errors in filtered position and speed. Parametric relations for P_{33}/σ_R^2, P_{13}/σ_R^2, and P_{23}/σ_R^2 have been determined but their utility is small compared to those shown in Figs. 3,

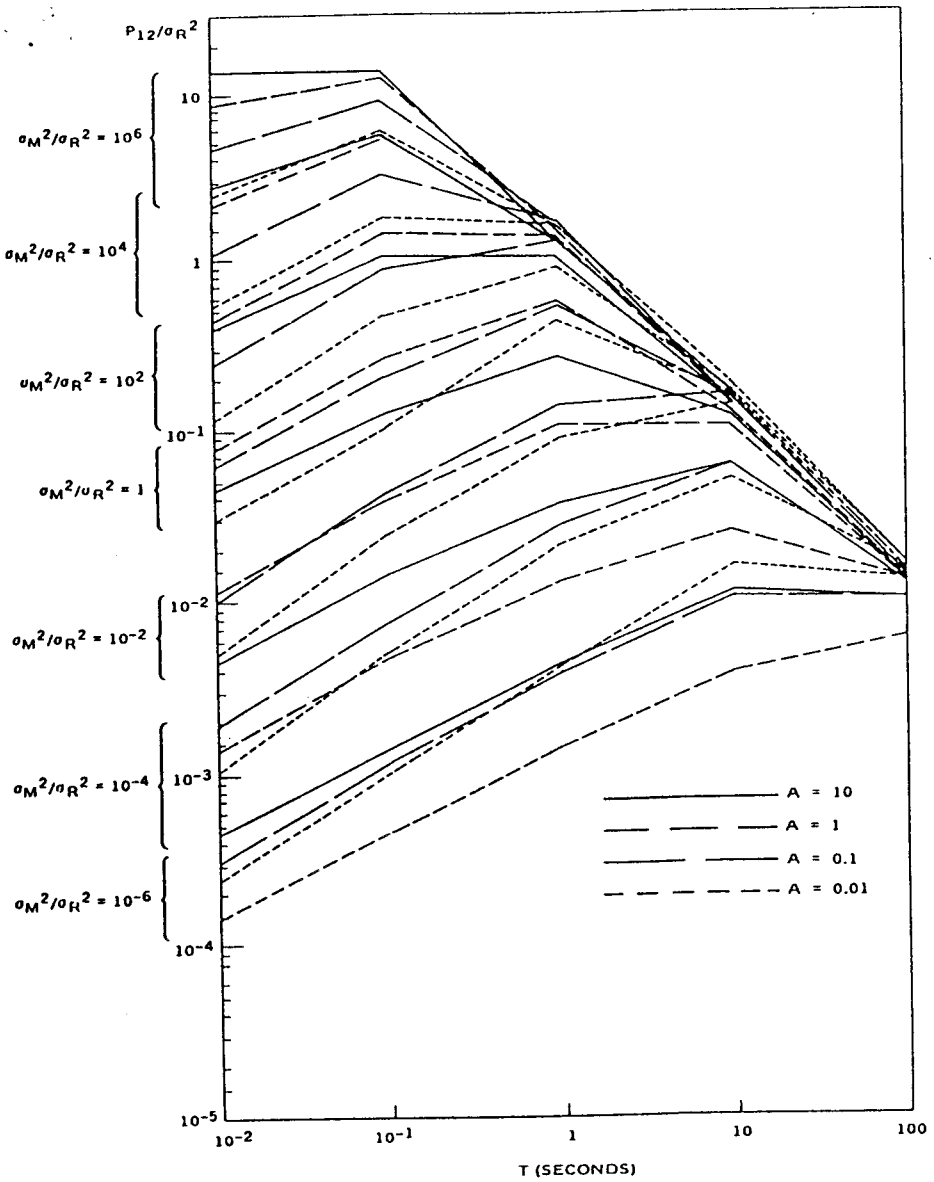

Fig. 5. Parametric behavior of P_{12}, the covariance of the filtered errors in position and velocity.

4, and 5, and have not been included in this paper.

These three figures can be extremely useful for providing a quick, first-cut estimate of the tracking performance for any system in which the sensor provides some combination of range, bearing, and elevation data. An example illustrates how these curves can be used to track maneuvering aircraft for an area defense application in which a radar provides measurements of range and bearing. The radar data rate is one sample per second ($T=1$), and the one sigma measurement accuracies are determined to be, for the aircraft at 10 nautical miles and after target cross section, environment, and sensor processing noise has been taken into account, 600 feet in range and 8 mrad in bearing. For the scenario considered, the aircraft moves at 1000 ft/s, can maneuver at a maximum of 4 g, and has a probability 0.2 of maneuvering at this rate and a probability 0.5 of not maneuvering at all. The average time constant of the maneuver class used in the scenario is found to be 10 seconds ($\alpha=0.1$). It is desired to determine the one-sigma accuracy in filtered range, bearing, and speed for this aircraft target when it is measured to be ten nautical miles from the tracking radar.

The tracking will be done in range and bearing coordinates using the Kalman filter described in this paper. Since the bearing and range measurement errors are independent, the filtering operation consists of decoupled tracking in range coordinates (range, range rate, and range acceleration) and bearing coordinates (bearing, rate, and bearing acceleration). In range coordinates

$$\sigma^2_{\text{M-range}} = \frac{(4 \times 32)^2}{3}(1 + 4(0.1) - 0.5) = 4920\ \text{ft}^2/\text{s}^4.$$

Hence

$$\sigma^2_{\text{M-range}}/\sigma^2_{\text{R-range}} = 49.2 \times 10^2/36 \times 10^4 = 1.36 \times 10^{-2}.$$

Using Figs. 3, 4, and 5 it follows (with $T=1$ and $\alpha=0.1$) that $P_{11}/\sigma_R^2=0.45$, $P_{22}/\sigma_R^2=0.095$, and $P_{12}/\sigma_R^2=0.15$.

ence $P_{11}(\text{range}) = 16.2 \times 10^4$ ft^2, $P_{22}(\text{range}) = 3.42 \times 10^4$ ft^2/s^4, and $P_{12}(\text{range}) = 5.3 \times 10^4$ ft^2/s^2. In bearing coordinates, $\sigma^2_{\text{M-bearing}} = \sigma^2_{\text{M-range}}/\text{range}^2 = 4920/(60\,000)^2 = 1.36 \times 10^{-6}$ so that $\sigma^2_{\text{M-bearing}}/\sigma^2_{\text{R-bearing}} = 1.36 \times 10^{-6}/(5 \times 10^{-3})^2 = 2.13 \times 10^{-2}$. Using Figs. 3, 4, and 5, it follows that $P_{11}/\sigma_R^2 = 0.47$, $P_{22}/\sigma_R^2 = 0.11$, $P_{12}/\sigma_R^2 = 0.17$. Hence $P_{11}(\text{bearing}) = 30.1 \times 10^{-6}$ rad^2, $P_{22}(\text{bearing}) = 7.03 \times 10^{-6}$ rad^2/s^4, and $P_{12}(\text{bearing}) = 10.85$ rad^2/s^2. The standard deviation of the filtered range accuracy is $\sqrt{P_{11}(\text{range})} = 402$ ft, and the standard derivation of the filtered bearing accuracy is $\sqrt{P_{11}(\text{bearing})} = 5.5$ mrad. The target speed v is given by $v = \sqrt{V_R^2 + R^2 v_\theta^2}$ where V_R is target range rate, R is target range, and v_θ is target bearing rate. Hence

$$\delta v = \frac{V_R \delta V_R + R v_\theta^2 \delta R + R^2 v_\theta \delta v_\theta}{v}.$$

The variance of the speed estimate is therefore

$$\sigma^2_{\text{speed}} = E(\delta v)^2 = \frac{1}{v^2}\Big[V_R^2 P_{22}(\text{range}) + R^2 v_\theta^4 P_{11}(\text{range}) + 2RV_R v_\theta^2 P_{12}(\text{range}) + R^4 v_\theta^2 P_{22}(\text{bearing})\Big].$$

This expression accounts for the independence of range and bearing errors, and treats δV_R, δR, and δv_θ as the errors in the filtered values of range rate, range, and bearing rate, respectively. For a 1000 ft/s target ($v = 1000$) moving on a course such that $V_R = Rv_\theta = 707$ ft/s, it follows that:

$$\sigma_{\text{speed}} = 0.707\sqrt{P_{22}(\text{range}) + v_\theta^2 P_{11}(\text{range}) + 2v_\theta P_{12}(\text{range}) + R^2 P_{22}(\text{bearing})}$$

$$= 0.707\sqrt{3.42 \times 10^4 + \left(\frac{707}{60\,000}\right)^2 (16.2 \times 10^4) + \frac{1414}{60\,000}(5.3 \times 10^4) + (60\,000)^2(7.03 \times 10^{-6})}$$

$$= 188 \text{ ft/s},$$

or 18.8 percent of the target speed.

The tracking accuracies associated with predicting target coordinates for a time S after receipt of the last data point can also be determined by the procedure developed here. The optimal prediction equations are, in each dimension,

$$\hat{X}(k + S/k) = \phi(S, \alpha)\hat{X}(k/k) \tag{26}$$

and the corresponding prediction error covariance matrix satisfies

$$P(k + S/k) = \phi(S, \alpha)P(k/k)\phi^T(S, \alpha) + Q(S, \alpha). \tag{27}$$

In this equation, the elements P_{11}, P_{12}, P_{22}, etc., of the covariance matrix for the filtered estimates of targets coordinates, etc. can be determined directly using Figs. 3, 4, and 5. The matrices $\phi(S, \alpha)$ and $Q(S, \alpha)$ are given by (13) and (19), and once calculated can be used to obtain the matrix $P(k+S/k)$. The elements of this matrix are then used as above to provide the statistics of the S-seconds-ahead target prediction errors.

VI. Tracking Accuracy Sensitivities

Figs. 3 and 4 illustrate the sensitivity of the errors in filtered position and velocity to the four primary tracking parameters: σ_R^2, σ_M^2, α, and T. As such they provide another important design tool to the tracking engineer who must frequently answer questions regarding tradeoffs between tracking accuracy and parameter value changes.

The data rate is the parameter most easily and therefore most frequently varied to improve tracking performance. The figures show that filtering accuracy increases as the data rate increases (T decreases), and that, in fact, as the data rate becomes unbounded ($T \to 0$), the filtering errors vanish. This occurs because for extremely short periods of time the target exhibits essentially straight line motion. Since with high data rates many measurements are received during these periods, the filter behaves as a least squares filter being used to track nonmaneuvering vehicles, and the tracking errors vanish. As the data rate decreases ($T \to \infty$), the uncertainties caused by target maneuver become increasingly important, and the tracking accuracy decreases. In the case of filtered velocity, the tracking errors increase without bound as T increases, primarily because during long periods of time, target maneuvers can result in very large changes of target speed. In the case of filtered position, the accuracy can decrease only to the level of the raw single-look measurement accuracy since this is the position uncertainty at receipt of each data point.

For prediction purposes, however, the benefits of reducing the data rate are not nearly so great. As (27) shows, when predicting a fixed time S ahead, the term $Q(S, \alpha)$ always appears in the prediction error covariance matrix $P(k + S/k)$ so that even if the data rate is increased to the point that the filtering error covariance matrix $P(k/k)$ vanishes, the prediction errors only reach a nonzero, often not small, lower limit. This result is particularly important for trajectory and orbit prediction calculations when fixed finite time period predictions are required, and must be taken into account before a data rate is selected.

The figures show that for the regions where filtering improves tracking performance ($P_{11}/\sigma_R^2 < 1$), the sensitivity of P_{11}/σ_R^2 to T is approximately a factor of 5 in P_{11}/σ_R^2 per decade of T. The sensitivity of P_{22}/σ_R^2 to T varies between a factor of 1.2/decade and 3 decades/

decade for T between 0.01 and 10. The sensitivity increases as the ratio σ_M^2/σ_R^2 increases.

The sensitivity of tracking performance to the correlation coefficient α is considerably smaller, indicating that errors in selecting α for a particular tracking application will not significantly degrade filter performance. The position and velocity errors vanish in the limit both as α decreases to zero and as α increases to infinity. The first case corresponds in the limit to a constantly accelerating target with no state excitation noise. The Kalman filter becomes equivalent to a least squares filter for such cases and the tracking errors vanish in the steady state. The second case corresponds to pure uncorrelated acceleration jitter that differs from white noise in that the acceleration correlation function consists of a finite spike, rather than a delta function, at the origin. Since the integral of this correlation function is zero, a situation similar to a constant velocity trajectory exists. Fig. 3 shows that the largest ratio between the maximum and minimum values of P_{11}/σ_R^2 is below 3 for any selected T and σ_M^2/σ_R^2, and for any α between 0.01 and 10. The corresponding ratio for P_{22}/σ_R^2 is found from Fig. 4 to be about 10 for $T \leq 10$. The relative insensitivity to α is therefore demonstrated.

The effects of changing the maneuver variance σ_M^2 are somewhat more pronounced. Increasing σ_M^2 increases tracking errors since it increases the likelihood that large changes in target position and speed will occur within a fixed time period. Fig. 3 shows that except for the upper region in the figure, increasing σ_M^2 by a factor of 100 increases P_{11}/σ_R^2 by a factor of approximately 2. The factor for P_{22}/σ_R^2 is more variable but is approximately 20. This greater sensitivity reflects the fact that acceleration variations have more pronounced an effect on vehicle speed than on vehicle position.

The sensitivity of the improvement ratios P_{11}/σ_R^2 and P_{22}/σ_R^2 to σ_R^2 can be determined exactly as the sensitivity to σ_M^2. In fact, decreasing σ_R^2 by a factor of 100 increases P_{11}/σ_R^2 by a factor of 2, and increases P_{22}/σ_R^2 by approximately 20. When σ_R^2 decreases by a factor of 100, therefore, P_{11} decreases by a factor of 50 and P_{22} by a factor of 5. Thus, although the improvement ratios worsen as the sensor noise becomes smaller, the tracking accuracy increases, as expected.

VII. Further Design Considerations

The tracking performance provided by the filter presented in this paper will often be below that obtained by simpler filters, such as least squares filters, when tracking maneuverable targets moving at constant velocity. This is the price paid in order to be able to track maneuvering targets well. Simple filters will often lose track of maneuvering targets while the filter presented here will not. The Kalman filter automatically keeps the gain vector relatively large in order to follow maneuvers as soon as they occur. Consequently, although performance against maneuvers is good, performance against nonmaneuvers, while good, is degraded from that of simpler filters. Since in most applications it is generally more critical not to lose track of maneuvering targets than it is to have superb performance against nonmaneuvering targets, the filter presented in this paper is a promising candidate for implementation. Often, simpler filters have maneuver detectors addended to them [6] in order to increase performance against maneuvers; however, these detectors increase the complexity of the filter and further analytical work must be completed in order to permit their performance to be properly analyzed and to allow sufficiently general design for wide classes of weapons systems tracking problems.

In most tactical weapons systems, the single parameter that can generally be selected to obtain desired tracking performance is the data rate (or, equivalently, the sampling interval T). The parameters σ_M^2 and α are determined by the target class to be tracked and are, therefore, outside the weapon system designers' control. The observation noise σ_R^2 consists of components due to target cross section, target range, natural and jamming environment, sensor frequency, and data processing techniques, only the last of which can be varied at will and even that can be done very infrequently because of other design and performance considerations more important than tracking accuracy. Figs. 3, 4, 5, and the analysis procedures discussed previously indicate how data rate selection can be made to obtain desired tracking performance. For instance, the inverse of the example presented in the last section would be the result that for the system described there and with tracking objectives being filtering standard deviations of 400 feet in range, 5.5 mrad in bearing, and 200 ft/s in speed for a 1000 ft/s target, a sampling interval of 1 second would be required.

VIII. Conclusions

It has been shown how, using a simple target model that accounts statistically for the magnitude and duration of target maneuvers, a Kalman filter suitable for implementation in tactical weapons systems can be constructed to optimally track maneuvering vehicles such as aircraft, ships, and submarines.

Parametric curves have been generated that permit the design engineer to quickly estimate the steady-state performance of this filter for any set of selected data rate, single look sensor measurement accuracies, encounter geometry, and class of maneuvering target when any sensor that provides some combination of range, bearing, and elevation measurements is being employed for the tracking function. An example is presented that illustrates how to perform such an estimation.

The sensitivity of tracking accuracy to data rate, maneuver magnitude, maneuver correlation coefficient, and single-look measurement accuracy is discussed, and it is indicated how this information can be of value to the system designer during tracking performance–parameter value selection tradeoffs.

More experience is required to determine the reliability and utility of the tracking approach presented here. Preliminary work using realistic Monte Carlo trajectory

simulations with a similar tracking filter indicate that the theoretical and empirical tracking accuracies agree to within about 30 percent.

Appendix I
Derivation of $Q(k)$

The maneuver excitation covariance matrix $Q(k)$ satisfies, using (15),

$$Q(k) = E[u(k)u^T(k)] = \int_{kT}^{(k+1)T}\int_{kT}^{(k+1)T}\begin{bmatrix} n_1(\tau) \\ n_2(\tau) \\ n_3(\tau) \end{bmatrix} \cdot [n_1(s)n_2(s)n_3(s)]2\alpha\sigma_M^2\delta(\tau - s)d\tau ds \quad (28)$$

$$2\alpha\sigma_M^2 \int_{kT}^{(k+1)T} \cdot \begin{bmatrix} n_1^2(\tau) & n_1(\tau)n_2(\tau) & n_1(\tau)n_3(\tau) \\ n_2(\tau)n_1(\tau) & n_2^2(\tau) & n_2(\tau)n_3(\tau) \\ n_3(\tau)n_1(\tau) & n_3(\tau)n_2(\tau) & n_3^2(\tau) \end{bmatrix} d\tau.$$

In this equation,

$$\begin{aligned}
n_1^2(\tau) &= \frac{1}{\alpha 4}\left[\exp\{-2\alpha[(k+1)T-\tau]\}+1\right. \\
&\quad -2\exp\{-\alpha[(k+1)T-\tau]\} \\
&\quad +\alpha^2[(k+1)T-\tau]^2-2\alpha[(k+1)T-\tau] \\
&\quad \left.+2\alpha[(k+1)T-\tau]\exp\{-\alpha[(k+1)T-\tau]\}\right] \\
n_1(\tau)n_2(\tau) &= \frac{1}{\alpha 3}\left[-\exp\{-2\alpha[(k+1)T-\tau]\}\right. \\
&\quad +2\exp\{-\alpha[(k+1)T-\tau]\}-\alpha[(k+1)T-\tau] \\
&\quad \cdot\exp\{-\alpha[(k+1)T-\tau]\} \\
&\quad \left.-1+\alpha[(k+1)T-\tau]\right] \qquad (29) \\
n_1(\tau)n_3(\tau) &= \frac{1}{\alpha 2}\left[-\exp\{-\alpha[(k+1)T-\tau]\}\right. \\
&\quad +\alpha[(k+1)T-\tau]\exp\{-\alpha[(k+1)T-\tau]\} \\
&\quad \left.+\exp\{-2\alpha[(k+1)T-\tau]\}\right] \\
n_2^2(\tau) &= \frac{1}{\alpha 2}\left[1-2\exp\{-\alpha[(k+1)T-\tau]\}\right. \\
&\quad \left.+\exp\{-2\alpha[(k+1)T-\tau]\}\right] \\
n_2(\tau)n_3(\tau) &= \frac{1}{\alpha}\left[\exp\{-\alpha[(k+1)T-\tau]\}\right. \\
&\quad \left.-\exp\{-2\alpha[(k+1)T-\tau]\}\right] \\
n_3^2(\tau) &= \exp\{-2\alpha[(k+1)T-\tau]\}.
\end{aligned}$$

Letting $Z=(k+1)T-\tau$, it follows that

$$Q(k) = 2\alpha\sigma_M^2 \int_0^T \begin{bmatrix} h_{11}(Z) & h_{12}(Z) & h_{13}(Z) \\ h_{12}(Z) & h_{22}(Z) & h_{23}(Z) \\ h_{13}(Z) & h_{23}(Z) & h_{33}(Z) \end{bmatrix} dZ \quad (30)$$

where

$$\begin{aligned}
h_{11}(Z) &= \frac{1}{\alpha^4}\left[e^{-2\alpha Z}+1-2e^{-\alpha Z}+\alpha^2Z^2-2\alpha Z+2\alpha Ze^{-\alpha Z}\right] \\
h_{12}(Z) &= \frac{1}{\alpha^3}\left[-e^{-2\alpha Z}+2e^{-\alpha Z}-\alpha Ze^{-\alpha Z}-1+\alpha Z\right] \\
h_{13}(Z) &= \frac{1}{\alpha^2}\left[-e^{-\alpha Z}+\alpha Ze^{-\alpha Z}+e^{-2\alpha Z}\right] \\
h_{22}(Z) &= \frac{1}{\alpha^2}\left[1-2e^{-\alpha Z}+e^{-2\alpha Z}\right] \\
h_{23}(Z) &= \frac{1}{\alpha}\left[e^{-\alpha Z}-e^{-2\alpha Z}\right] \\
h_{33}(Z) &= e^{-2\alpha Z}. \qquad (31)
\end{aligned}$$

Utilizing the identities

$$\begin{aligned}
&\int_0^T dZ = T, \quad \int_0^T e^{-\alpha Z}dZ = \frac{1-e^{-\alpha T}}{\alpha}, \\
&\int_0^T e^{-2\alpha Z}dZ = \frac{1-e^{-2\alpha T}}{2\alpha}, \quad \int_0^T \alpha Z dZ = \frac{\alpha T^2}{2} \\
&\int_0^T \alpha^2 Z^2 dZ = \frac{\alpha^2 T^3}{3}, \qquad (32) \\
&\int_0^T \alpha Z e^{-\alpha Z}dZ = \frac{1}{\alpha}\left[1-e^{-\alpha T}-\alpha Te^{-\alpha T}\right]
\end{aligned}$$

it follows that

$$Q(k) = 2\alpha\sigma_M^2 \begin{bmatrix} q_{11} & q_{12} & q_{13} \\ q_{12} & q_{22} & q_{23} \\ q_{13} & q_{23} & q_{33} \end{bmatrix} \quad (33)$$

where

$$\begin{aligned}
q_{11} &= \frac{1}{\alpha^4}\left[\frac{1-e^{-2\alpha T}}{2\alpha}+T-2\frac{1-e^{-\alpha T}}{\alpha}+\frac{\alpha^2T^3}{3}\right. \\
&\quad \left.-\alpha T^2+\frac{2}{\alpha}\left[1-e^{-\alpha T}-\alpha Te^{-\alpha T}\right]\right] \\
&= \frac{1}{2\alpha^5}\left[1-e^{-2\alpha T}+2\alpha T+\frac{2\alpha^3T^3}{3}\right. \\
&\quad \left.-2\alpha^2T^2-4\alpha Te^{-\alpha T}\right] \\
q_{12} &= \frac{1}{\alpha^3}\left[\frac{e^{-2\alpha T}-1}{2\alpha}-2\frac{e^{-\alpha T}-1}{\alpha}\right. \\
&\quad -\frac{1}{\alpha}\left[-\alpha Te^{-\alpha T}-e^{-\alpha T}+1\right] \\
&\quad \left.-T+\frac{\alpha T^2}{2}\right] \\
&= \frac{1}{2\alpha^4}\left[e^{-2\alpha T}+1-2e^{-\alpha T}+2\alpha Te^{-\alpha T}\right. \\
&\quad \left.-2\alpha T+\alpha^2T^2\right] \\
q_{13} &= \frac{1}{\alpha^2}\left[\frac{1-e^{-2\alpha T}}{2\alpha}+\frac{e^{-\alpha T}-1}{\alpha}\right. \\
&\quad \left.+\frac{1}{\alpha}\left[1-e^{-\alpha T}-\alpha Te^{-\alpha T}\right]\right] \\
&= \frac{1}{2\alpha^3}\left[1-e^{-2\alpha T}-2\alpha Te^{-\alpha T}\right]
\end{aligned}$$

$$q_{22} = \frac{1}{\alpha^2}\left[\frac{1 - e^{-2\alpha T}}{2\alpha} + 2\frac{e^{-\alpha T} - 1}{\alpha} + T\right]$$

$$= \frac{1}{2\alpha^3}\left[4e^{-\alpha T} - 3 - e^{-2\alpha T} + 2\alpha T\right]$$

$$q_{23} = \frac{1}{\alpha}\left[\frac{e^{-2\alpha T} - 1}{2\alpha} - \frac{e^{-\alpha T} - 1}{\alpha}\right]$$

$$= \frac{1}{2\alpha^2}\left[e^{-2\alpha T} + 1 - 2e^{-\alpha T}\right]$$

$$q_{33} = \frac{1}{2\alpha}\left[1 - e^{-2\alpha T}\right]. \tag{34}$$

Appendix II
Kalman Filter Covariance Initialization Equations

The estimation errors resulting from using (23) to initialize the filter state estimation equations are:

$$\begin{aligned}
\varepsilon_1(1\,1) &= x_1(1) - \hat{x}_1(1/1) = x_1(1) - x_1(1) - v(1) \\
&= -v(1) \\
\varepsilon_2(1\,1) &= x_2(1) - \hat{x}_2(1/1) \\
&= x_2(0) + \frac{1}{\alpha}\left[1 - e^{-\alpha T}\right]x_3(0) \\
&\quad + u_2(0) - \frac{x_1(1) + v(1) - x_1(0) - v(0)}{T} \\
&= \frac{v(0)}{T} - \frac{v(1)}{T} + \left[\frac{-e^{-\alpha T}}{\alpha} + \frac{1}{\alpha^2 T} - \frac{e^{-\alpha T}}{\alpha^2 T}\right] \\
&\quad \cdot x_3(0) + u_2(0) - \frac{u_1(0)}{T} \\
\varepsilon_3(1\,1) &= x_3(1) - \hat{x}_3(1/1) = e^{-\alpha T}x_3(0) + u_3(0).
\end{aligned} \tag{35}$$

Hence, since

$$P_{ij}(1/1) = E\left[\varepsilon_i(1/1)\varepsilon_j'(1/1)\right],$$

it follows that

$$\begin{aligned}
P_{11}(1/1) &= \sigma_R^2 \\
P_{12}(1/1) &= \sigma_R^2/T \\
P_{13}(1/1) &= 0 \\
P_{22}(1/1) &= \frac{2\sigma_R^2}{T^2} + \frac{\sigma_M^2}{\alpha^4 T^2}\left[1 - e^{-\alpha T} - \alpha T e^{-\alpha T}\right]^2 \\
&\quad + Eu_2^2 + \frac{Eu_1^2}{T^2} - \frac{2}{T}Eu_1u_2 \\
&= \frac{2\sigma_R^2}{T^2} + \frac{\sigma_M^2}{\alpha^4 T^2} \\
&\quad \cdot \left[2 - \alpha^2 T^2 + \frac{2\alpha^3 T^3}{3} - 2e^{-\alpha T} - 2\alpha T e^{-\alpha T}\right] \\
P_{23}(1/1) &= \frac{\sigma_M^2}{\alpha^2 T}\left[e^{-\alpha T} - \alpha T e^{-2\alpha T} - e^{-2\alpha T}\right] \\
&\quad + Eu_2u_3 - \frac{Eu_1u_3}{T} \\
&= \frac{\sigma_M^2}{\alpha^2 T}\left[e^{-\alpha T} + \alpha T - 1\right] \\
P_{33}(1/1) &= \sigma_M^2 e^{-2\alpha T} + Eu_3^2 = \sigma_M^2 e^{-2\alpha T} \\
&\quad + \sigma_M^2\left[1 - e^{-2\alpha T}\right] = \sigma_M^2.
\end{aligned} \tag{36}$$

References

[1] L. A. Wan, R. A. Singer, and R. A. Monzingo, "Optimal tracking and prediction of dynamic targets," *Proc. First NIKE-X Control, Guidance and Intercept Symp.*, (Redstone Arsenal, Huntsville, Ala., July 1967).

[2] R. A. Singer and K. W. Behnke, "Tracking filter selection for aerospace applications," to be presented at Kyoto Internatl. Conf. on Circuit and Sys. Theory, Kyoto, Japan, September 9–11, 1970.

[3] N. Wiener, *Extrapolation, Interpolation, and Smoothing of Stationery Time Series*. New York: Wiley, 1949.

[4] J. T. Tou, *Optimal Design of Digital Control Systems*. New York: Academic Press, 1963.

[5] A. J. Kanyuck, "Transient response of tracking filters with randomly-interrupted data," *IEEE Trans. Aerospace and Electronic Systems*, vol. AES-6, pp. 313–323, May 1970.

[6] H. P. Semmelhack and S. G. Hoppe, "Modern techniques for automatic track-while-scan," *Proc. Second Hawaii Internatl. Conf. on System Sciences* (Honolulu, Hawaii), January 1969.

Robert A. Singer (S'63–M'68) was born in Bronx, N. Y., on December 8, 1942. He received the B.E.S. degree from Rensselaer Polytechnic Institute, Troy, N. Y., in 1964, and the M.S.E.E. and Ph.D. degrees from Stanford University, Stanford, Calif., in 1965 and 1968.

As a Howard Hughes Doctoral Fellow, from 1965 to 1967, he was involved in applications of Kalman filtering and estimation theory to ballistic and aerodynamic target tracking. He participated as well in analyses of fusing techniques and warhead capabilities. Head of the Advanced Studies Group at Hughes Aircraft Company, Fullerton, Calif., he is now concerned with the control, guidance, estimation, and dynamic characteristics of a variety of ballistic, air supported, and underwater weapons systems.

Dr. Singer is a member of Tau Beta Pi, Sigma Xi, and the American Meteorological Society.